Marine Environmental Research 79 (2012) 142–151

Contents lists available at SciVerse ScienceDirect

Marine Environmental Research

journal homepage: www.elsevier.com/locate/marenvrev

Physiological responses of the marine diatom *Thalassiosira pseudonana* to increased pCO_2 and seawater acidity

Guiyuan Yang, Kunshan Gao*

State Key Laboratory of Marine Environmental Science, Xiamen University, Daxue Road 182 (HAIYANG-LOU), Xiamen, Fujian 361005, China

ARTICLE INFO

Article history:
Received 27 June 2011
Received in revised form
25 May 2012
Accepted 2 June 2012

Keywords:
CCM
CO_2
Chlorophyll fluorescence
Diatom
Growth
Ocean acidification
Photosynthesis
Respiration
Thalassiosira pseudonana

ABSTRACT

We studied the effects of elevated CO_2 concentration and seawater acidity on inorganic carbon acquisition, photoinhibition and photoprotection as well as growth and respiration in the marine diatom *Thalassiosira pseudonana*. After having grown under the elevated CO_2 level (1000 μatm, pH 7.83) at subsaturating photosynthetically active radiation (PAR, 75 μmol photons m^{-2} s^{-1}) for 20 generations, photosynthesis and dark respiration of the alga increased by 25% (14.69 ± 2.55 fmol C $cell^{-1}$ h^{-1}) and by 35% (4.42 ± 0.98 fmol O_2 $cell^{-1}$ h^{-1}), respectively, compared to that grown under the ambient CO_2 level (390 μatm, pH 8.16), leading to insignificant effects on growth (1.09 ± 0.08 d^{-1} *v* 1.04 ± 0.07 d^{-1}). The photosynthetic affinity for CO_2 was lowered in the high-CO_2 grown cells, reflecting a down-regulation of the CO_2 concentrating mechanism (CCM). When exposed to an excessively high level of PAR, photochemical and non-photochemical quenching responded similarly in the low- and high-CO_2 grown cells, reflecting that photoinhibition was not influenced by the enriched level of CO_2. In *T. pseudonana*, it appeared that the energy saved due to the down-regulated CCM did not contribute to any additional light stress as previously found in another diatom *Phaeodactylum tricornutum*, indicating differential physiological responses to ocean acidification between these two diatom species.

1. Introduction

The oceans are taking up over one million tons of CO_2 per h and have been acidified by 30% since the industrial revolution, and will be further acidified by 150% (pH drop to 7.8) by the end of this century (Caldeira and Wickett, 2003; IPCC, 2001), leading to ocean acidification. Typical chemical changes associated with the ocean acidification are increased concentrations of pCO_2, H^+ and HCO_3^- and decreased concentration of CO_3^{2-} and the $CaCO_3$ saturation state. Reduction of pH in seawater can affect the intracellular acid-base balance or the energy demand to maintain the balance and, therefore, membrane electrochemical potential and enzyme activity may be influenced (Kramer et al., 2003; Milligan et al., 2009). At the same time, elevated CO_2 levels can influence inorganic carbon (Ci) acquisition of phytoplankton (Burkhardt et al., 2001; Trimborn et al., 2009), resulting in changes in growth rate and primary productivity (see the review by Riebesell and Tortell, 2011 and references therein). A number of studies show stimulative effects on phytoplankton primary productivity (Hein and Sand-Jensen, 1997; Riebesell and Tortell, 2011), while unaffected (Boelen et al., 2011; Nielsen et al., 2012, 2010; Tortell et al., 2002, 2000; Tortell and Morel, 2002) and negative effects (Feng et al., 2009; Low-DÉCarie et al., 2011; Torstensson et al., 2012) of ocean acidification have also been observed.

Diatoms are responsible for about 40% of the total primary production in the oceans. The half-saturation ($K_{1/2}$) CO_2 concentration for carboxylation catalyzed by Rubisco is suggested to range from 31 to 41 μmol L^{-1} CO_2 (Badger et al., 1998), about three to four times higher than the ambient CO_2 concentration of seawater. Theoretically, photosynthesis and growth of diatom species can be limited by the availability of CO_2 (Riebesell et al., 1993), and oceanic primary production might be enhanced by increasing atmospheric CO_2 concentration (Hein and Sand-Jensen, 1997; Riebesell and Tortell, 2011; Schippers et al., 2004). However, the growth rate of diatom-dominated phytoplankton assemblages is not affected by an elevated CO_2 concentration of 800 μatm, although changes occur in cellular biochemistry (Tortell et al., 2000). Growth of *Skeletonema costatum* is not stimulated by enriched CO_2 concentration (800 μatm) under laboratory conditions (Chen and Gao, 2003), but it is enhanced in a mesocosm at an elevated CO_2 concentration of 750 μatm (Kim et al., 2006). Growth of the diatoms *Phaeodactylum tricornutum* (Wu et al., 2010), *Navicula pelliculosa* (Low-DÉCarie

* Corresponding author. Tel.: +86 592 2187982; fax: +86 592 2187963.
E-mail addresses: yanggy004@163.com (G. Yang), ksgao@xmu.edu.cn (K. Gao).

0141-1136/$ – see front matter © 2012 Elsevier Ltd. All rights reserved.
http://dx.doi.org/10.1016/j.marenvres.2012.06.002

et al., 2011) and *Attheya* sp. (King et al., 2011) is also enhanced under elevated CO_2 levels under laboratory conditions. These controversial findings reflect differential physiological responses among different species or different experimental conditions. Obviously, more work is needed to explore the mechanistic responses of different diatom species to ocean acidification. Although photosynthesis of diatoms is likely to be stimulated by increased availability of CO_2, lower pH might enhance their respiration too (Wu et al., 2010), which would down-regulate their contribution to the marine biological CO_2 pump. However, little is known on this aspect.

Most diatoms operate CO_2 concentrating mechanisms (CCMs) to supply CO_2 to the proximity of Rubisco, which exhibits active transport of CO_2 and/or HCO_3^- across the cellular membrane. Different algal species or growth conditions show differential preferences to CO_2 or HCO_3^- (Burkhardt et al., 2001; Nimer et al., 1997). For example, *Thalassiosira punctigera* exclusively use free CO_2 (Elzenga et al., 2000), while *Thalassiosira pseudonana* can take up both CO_2 and HCO_3^- (Trimborn et al., 2009), which can be directly transported across the cell membrane without extracellular catalysis by periplasmic carbonic anhydrase (eCA) (Elzenga et al., 2000; Nimer et al., 1997). Both eCA and intracellular CA (iCA) accelerate the inter-conversion of CO_2 and HCO_3^- and facilitate Ci acquisition (Silverman, 1991). The activity of eCA can be down-regulated under elevated CO_2 concentrations relevant to climate change (Burkhardt et al., 2001; Chen and Gao, 2003; Martin and Tortell, 2008; Matsuda et al., 2001; Rost et al., 2003), therefore, active transport or use of HCO_3^- would be reduced. *Thalassiosira weissflogii* operates a C_4-like pathway to concentrate intracellular Ci, which is stored as an organic C_4 carbon compound (malic or aspartic acid) with the catalysis of phosphoenolpyruvate carboxylase (PEPCase) prior to fixation by Rubisco (Reinfelder et al., 2000, 2004); and *T. pseudonana* may also operate such C_4 pathway since it has the genes of PEPCase and phosphoenolpyruvate carboxykinase (PEPCKase) (Armbrust et al., 2004). Operation of CCMs is energy-dependent, because active transport of CO_2 and/or HCO_3^- (Li and Canvin, 1998), biosynthesis of CA and PEPCase (Bouma et al., 1994) and maintaining higher cellular Ci concentration by counteracting CO_2 efflux (Sukenik et al., 1997; Tchernov et al., 1997) are all costly. From this point of view, the energy saved from the down-regulated CCM of phytoplankton may stimulate their growth under elevated levels of CO_2 when photosynthesis is light limited (Wu et al., 2010).

On the other hand, down-regulated CCMs might cause additional light stress (Wu et al., 2010). Previously, energy delivered from photochemical processes was suggested to fuel active transport of CO_2 and HCO_3^- (Li and Canvin, 1998; Sültemeyer et al., 1993; Sukenik et al., 1997). The major energy expended by the CCMs in diatoms is in active Ci transport (Hopkinson et al., 2011). Doubling of the atmospheric CO_2 level would save about 20% of the energy demand for CCMs of diatoms such as *T. weissflogii*, *T. pseudonana*, *Thalassiosira oceanica* and *P. tricornutum* (Hopkinson et al., 2011). Such saved light energy might lead to additional light stress and cause photoinhibition (Wu et al., 2010). It is possible that the observed effects of ocean acidification on different diatom species depend on the balance between the down-regulated and up-regulated physiological processes due to increased CO_2 availability and changes in seawater chemistry. The aim of this study was to examine the effect of ocean acidification on growth, photosynthesis, dark respiration, Ci acquisition, photosynthetic electron transport, photoinhibition and photoprotection of *T. pseudonana* when acclimated to elevated CO_2/low pH conditions. We found that the enrichment of CO_2 to 1000 μatm with the reduction of pH to 7.83 enhanced photosynthetic carbon fixation and mitochondrial respiration but result insignificant changes in growth rate or photoinhibition.

2. Materials and methods

2.1. Culture conditions

Thalassiosira pseudonana (CCMP 1335) was inoculated in natural seawater collected from the pelagic South China Sea (18° N, 111° E), which had been autoclaved and enriched with Aquil medium (Morel et al., 1979). This species is a model diatom with whole genome known (Armbrust et al., 2004). The strain used in this study is recognized to have been maintained under indoor conditions for decades. Nevertheless, physiological studies after the strain's acclimation to ocean acidification condition still can provide some species-level knowledge. The cells were grown in 500-mL Erlenmeyer flask in a plant growth CO_2 chamber (HP1000G-D, Ruihua, China) at 20 ± 0.1 °C with a 12 h:12 h light:dark cycle. Cultures were illuminated at 75 μmol photons m^{-2} s^{-1} (a sub-saturating photosynthetically active radiation (PAR) intensity) provided by cool-white fluorescent lamps. By partially renewing the culture medium every 24 h (at the end of the light period), cell concentration was controlled within a range of 0.7×10^5 to 2.5×10^5 cell mL^{-1} (exponential growth phase) for 10 generations before being used for the CO_2 perturbation experiment. Cells were counted using a Coulter Z2 Particle Count and Size Analyzer (Beckman Coulter Inc., Fullerton, CA, USA), before and after renewal of the medium, every 24 h.

Two levels of CO_2 concentration, 390 μatm (outdoor ambient air) and 1000 μatm (projected for the end of this century according to IPCC, 2001), were prepared in two separate plant growth CO_2 chambers, where the CO_2 perturbation experiment was carried out. The enriched CO_2 level was a mixture of outdoor ambient air and pure CO_2, automatically controlled by continuous CO_2-sensing and controlling systems equipped with the CO_2 chamber, leading to a variation in the CO_2 concentration of less than 5%. Culture conditions (e.g. culture vessel, temperature, growth light intensity, light:dark cycle, cell concentration) for the CO_2 perturbation treatment were the same as mentioned above. The cultures were aerated to achieve an ocean acidification condition with 0.22-μm-filtered target gases at a flow rate of 350 mL min^{-1}, and diluted with pre-CO_2-equilibrated medium, so that stable pH levels were sustained during the culture (Table 1). Triplicate cultures were run for each CO_2 treatment. All the experiments were carried out using the cells that had acclimated to CO_2 perturbation for at least 20 generations.

After being acclimated to the two CO_2 levels for more than 20 generations, specific growth rate (μ, d^{-1}) of *T. pseudonana* was determined based on the change in cell concentrations over 24 h. For measurement of the photosynthetic pigment contents, cells of each culture were collected on 25-mm diameter GF/F filter (Whatman Inc., Piscataway, NJ, USA), extracted in the dark for 4 h with pure methanol at room temperature (Lloyd and Tucker, 1988), and measured spectrophotometrically using a DU800 spectrophotometer (Beckman Coulter Inc., Fullerton, CA, USA). The concentrations of chlorophyll *a* (Chl. *a*) and chlorophyll *c* (Chl. *c*) were calculated according to Ritchie (2006).

2.2. Determination of seawater carbonate chemistry

Dissolved inorganic carbon (DIC) and pH were measured prior to and after the daily dilution as well as at the middle of the light period to assure the stability of the carbonate system in culture. DIC was measured using an automatic system (AS-C3, Apollo SciTech Inc., Bogart, GA, USA) involving an infrared gas detector (Li-Cor 7000, Li-Cor) after the samples were filtered into a syringe without any water–air CO_2 exchange. Samples (0.5 mL) were acidified using phosphoric acid, and any subsequently released CO_2 was quantified

Table 1
Carbonate chemistry parameters at the end of the light period (After), in the middle of the light period (Mid) and 24 h later before the dilution of the medium (Prior) for low-CO_2 (LC, pH 8.16, upper line) and high-CO_2 (HC, pH 7.83, lower line) cultures. Total dissolved inorganic carbon (DIC), pH_{NBS}, nutrient concentration, temperature (20 °C) and salinity (35) were used to calculate other parameters by running the CO_2 system analyzing software (CO2SYS). TA stands for total alkalinity. These parameters were averaged from three replicate measurements. The values are means ± SD. Different superscripted letters represent significant difference between the ambient and acidified conditions.

	pH_{NBS}	DIC (μmol kg^{-1})	HCO_3^- (μmol kg^{-1})	CO_3^{2-} (μmol kg^{-1})	CO_2 (μmol kg^{-1})	TA (μmol kg^{-1})
After	8.16 ± 0.01[a]	2041.1 ± 4.1[a]	1832.6 ± 1.7[a]	195.1 ± 2.8[a]	13.4 ± 0.1[a]	2332.2 ± 8.0[a]
	7.83 ± 0.02[b]	2221.0 ± 10.2[b]	2084.4 ± 13.1[b]	103.9 ± 4.9[b]	32.7 ± 1.9[b]	2348.3 ± 2.9[a]
Mid	8.16 ± 0.01[a]	2048.0 ± 3.6[a]	1838.7 ± 1.2[a]	195.8 ± 5.0[a]	13.5 ± 0.3[a]	2319.9 ± 2.4[a]
	7.85 ± 0.01[b]	2205.8 ± 5.3[b]	2068.2 ± 5.9[b]	106.2 ± 1.1[b]	31.5 ± 0.5[b]	2338.0 ± 3.1[a]
Prior	8.16 ± 0.01[a]	2036.5 ± 8.5[a]	1829.7 ± 7.0[a]	193.3 ± 4.5[a]	13.5 ± 0.4[a]	2315.2 ± 13.1[a]
	7.82 ± 0.01[b]	2181.7 ± 7.1[b]	2050.0 ± 8.8[b]	98.3 ± 3.0[b]	33.4 ± 1.3[b]	2301.0 ± 1.3[a]

with an infrared CO_2 detector (Cai and Wang, 1998). The pH value was measured using a DL15 Titrator (Mettler-Toledo, Schwerzenbach, Switzerland), which was calibrated (3 point calibration) every day with standard NBS (National Bureau of Standards, USA standard) buffer solution (Hanna). Parameters of the carbonate system were calculated from the known value of DIC, pH, salinity, silicate, phosphate and temperature using the CO2SYS software (Lewis and Wallace, 1998). Equilibrium and dissociation constants for carbonic acid and boric acid were chosen according to Roy et al. (1993) and Dickson (1990), respectively.

2.3. Determination of photosynthesis and respiration rates

In the middle of the light period, cells were gently collected onto 50-mm diameter nitrocellulose membranes (0.22-μm pore-size, Xinya, China) under low pressure (<0.2 MPa, no ruptured cells were microscopically observed), washed off and re-suspended in 50 mmol L^{-1} Tris buffered medium (Tortell et al., 2000), which was pre-equilibrated with the target CO_2 gases, and the pH levels were adjusted by adding hydrochloric acid or sodium hydroxide to equate with their growth levels (7.83 and 8.16 for the high- and low-CO_2 grown cells, respectively). Cell suspensions with a final concentration of ca. 1.5×10^5 cell mL^{-1} were dispensed into 15-mL quartz tubes, incubated with 100 μL–5 μCi (0.185 MBq) of ^{14}C-labeled sodium bicarbonate (ICN Radiochemicals, Irvine, CA, USA) under a halogen lamp (which emits a small amount of UV irradiance). All the tubes, wrapped with Ultraphan 395 foil (UV Opak, Digefra, Munich, Germany) to cut off UV radiation, were placed in a water bath for temperature control at 20 ± 0.1 °C using a circulating cooler (CTP-3000, Eyela, Tokyo, Japan). Different layers of neutral density screen were adopted to achieve seven levels of PAR intensity (15, 33, 46, 111, 191, 348 and 600 μmol photons m^{-2} s^{-1}), and tubes wrapped with aluminum foil were incubated as the dark control. Triplicate tubes for each PAR level were incubated for 20 min (no significant change of pH was observed during 20 min incubation). After incubation, cells were filtered onto Whatman GF/F filters (25 mm), which were placed into 20-mL scintillation vials and exposed to HCl fumes overnight, then dried (50 °C, 6 h) to expel non-fixed labeled carbon (Gao et al., 2007). Radioactivity of the fixed ^{14}C was counted with a liquid scintillation counter (Tri-Carb 2800TR, Perkin–Elmer, Waltham, USA) after adding 3 mL scintillation cocktail (Hisafe 3, Perkin–Elmer) to each vial. The rate of photosynthetic carbon fixation was calculated according to Holm-Hansen and Helbling (1995).

For measurement of dark respiration, cells were harvested and re-suspended as above with a final concentration of ca. 2.5×10^6 cell mL^{-1} in a 20-mL tube, which was placed in a water-jacketed chamber for temperature control (20 ± 0.1 °C). Dark acclimation for 10 min was applied to eliminate the effect of post-illumination of low PAR intensity on dark respiration before measurement (Beardall et al., 1994). Respiratory O_2 removal was measured using a Clark-type oxygen electrode (5300A, Yellow Springs Instruments, USA) in darkness for 10 min. Since the cultures were maintained axenically, no O_2 consumption was detected in the medium after filtering off the cells with 0.22-μm pore-size membrane, indicating that bacteria did not contribute to the O_2 removal.

2.4. Fluorescence measurements

Chlorophyll *a* fluorescence is a powerful indicator for the properties of the photosynthetic apparatus. To assess the photochemical responses of the cells to the changes in the seawater carbonate system, we measured the rapid light curve (RLC), photochemical quantum yield (Φ_{PSII}), non-photochemical quenching (NPQ) and the effective absorption cross-section of the photosystem II (PSII) reaction centers (σ_{PSII}, nm^2 $PSII^{-1}$) using a Xenon-Pulse Amplitude Modulated fluorometer (XE-PAM, Walz, Germany) or a Fluorescence Induction and Relaxation system (FIRe, Satlantic, Halifax, Canada). Cells were collected, washed and re-suspended in 50 mmol L^{-1} Tris buffer medium with an approximate concentration of 0.5×10^5 cell mL^{-1}. Low-CO_2 grown cells re-suspended in low-CO_2 buffer were named LC cells, while if they were re-suspended in high-CO_2 buffer then they were named LC–HC cells. The similar definitions were applied to HC and HC–LC cells. The XE-PAM displays superiority in measuring RLC (Gordillo et al., 2001; Ihnken et al., 2010) and was chosen for RLC determination in the present study. Before measurement of RLC, the re-suspended cells were incubated at 75 μmol photons m^{-2} s^{-1} and 20 °C for 10 min to avoid induction effects on the photosystems caused by quasi-dark adaptation during manipulation. The RLC is the relative electron transport rate (rETR) in response to eight different, and increasing actinic, PAR intensities, with a 10 s duration for each increment separated by a 0.8 s saturating pulse (4000 μmol photons m^{-2} s^{-1}). The rETR (an arbitrary unit) was calculated as: $rETR = \Phi_{PSII} \times 0.5 \times PFD$, where Φ_{PSII} is the photochemical quantum yield of PSII in light, PFD is the actinic PAR intensity (μmol photons m^{-2} s^{-1}), and the factor 0.5 accounts for approximately 50% of all the absorbed energy allocated to PSII. To simultaneously examine Φ_{PSII}, NPQ and σ_{PSII} in response to excessive PAR levels, the FIRe was chosen since it was not possible to obtain σ_{PSII} with XE-PAM. The cells were dark acclimated for 15 min before being exposed to growth light intensity (75 μmol photons m^{-2} s^{-1}) or excessive PAR levels (1200 μmol photons m^{-2} s^{-1}). The photochemical quantum yield was calculated as $\Phi_{PSII} = (F_m - F_0)/F_m$ for dark-adapted cells or $\Phi_{PSII} = (F_m' - F_t)/F_m'$ for light-adapted cells, where F_m and F_m' are the maximum chlorophyll fluorescence yields in the dark-adapted and the light-adapted states, respectively; F_0 the minimal chlorophyll fluorescence yield in the dark-adapted state; and F_t the steady fluorescence level in light-adapted state. NPQ was calculated as: $NPQ = (F_m - F_m')/F_m'$. Since the absolute values of the photochemical yield differ by about 15% between XE-PAM and FIRe techniques (Falkowski et al., 2004), comparisons were always made for the data obtained from the same device.

2.5. Determination of photosynthetic inorganic carbon affinity

Photosynthetic affinity for CO_2, reflecting an operational efficiency of the CCM, was determined using either the PSII fluorescence technique (Wu et al., 2010) or the ^{14}C-labeling technique. In order to compare their Ci acquisition capability, the photosynthetic carbon fixation and electron transport rates were measured as a function of DIC concentration at the same pH level of 8.16 for the high- and low-CO_2 grown cells. The collected cells were re-suspended at ca. 1.5×10^5 cell mL^{-1} in DIC-free medium buffered with 50 mmol L^{-1} Tris. Exhaustion of intracellular Ci was obtained by incubating the cells in DIC-free solution for less than 20 min before each measurement. Both photosynthesis *v* DIC and rETR *v* DIC curves were determined with different samples in freshly prepared media of different DIC levels (that is, bicarbonate was not added consecutively into the same bottle). For photosynthesis *v* DIC curves, ^{14}C labeled sodium bicarbonate was added in the same amount as mentioned above and incubated under a photosynthesis-saturated PAR level of 400 μmol photons m^{-2} s^{-1} for 20 min. While for rETR *v* DIC curves, the steady yield of rETR for each DIC level (eight levels) was obtained within 3 min at actinic light of 400 μmol photons m^{-2} s^{-1}.

2.6. Data analysis

Significant differences among treatments were analyzed using One-way ANOVA and the Tukey test (confidence level $p = 0.05$). The photosynthesis *v* irradiance curves (P–I curves) were fitted following the model, $P = P_{max} \times \tanh(\alpha \times I/P_{max})$ (Jassby and Platt, 1976), where P is the photosynthetic rate normalized to cell concentration (fmol C $cell^{-1}$ h^{-1}), P_{max} is the maximum photosynthetic rate, α is the apparent photosynthetic efficiency, and I is the PAR intensity. I_k, the PAR intensity at which photosynthesis is initially saturated, was calculated as P_{max}/α. The RLCs were analyzed in the same way. The photosynthesis *v* DIC and rETR *v* DIC curves were fitted according to the Michaelis–Menten formula: $V = V_{max} \times S/(K_{1/2} + S)$, from which the corresponding kinetic parameters of half-saturation constants ($K_{1/2}$) and the maximum rates (V_{max}) for photosynthesis and relative electron transport were derived. The ratio of V_{max} to $K_{1/2}$ was used to evaluate the capacity for Ci acquisition or carboxylation (Xu and Gao, 2009), which reflects that with the same $K_{1/2}$ value, cells with higher V_{max} possess higher efficiency of Ci acquisition or carboxylation.

3. Results

3.1. Carbonate chemistry system

Carbonate chemistry parameters under the simulated ocean acidification condition were representative of those projected for the end of this century (Table 1). Enriched CO_2 concentration in air to 1000 μatm significantly increased DIC, HCO_3^- and CO_2 in the medium by 7.87%, 12.7% and 141%, whereas it decreased pH and CO_3^{2-} by 0.33 and by 47%, respectively. The total alkalinity (TA) remained unchanged.

3.2. Growth rate and pigment content

After acclimation to the target carbonate chemistry system for 20 generations, no significant difference was observed in growth rate, cellular contents of Chl. *a* and Chl. *c* between the high- (HC, 1000 μatm) and ambient (low)-CO_2 (LC, 390 μatm) grown cells ($p > 0.1$). Growth rate was 1.09 ± 0.08 d^{-1} and 1.04 ± 0.07 d^{-1} for HC and LC cells, respectively. The contents of Chl. *a* were 0.166 ± 0.009 pg $cell^{-1}$ in the HC and 0.176 ± 0.014 pg $cell^{-1}$ in the LC cells, that of Chl. *c* were 0.038 ± 0.008 pg $cell^{-1}$ in the HC and 0.036 ± 0.007 pg $cell^{-1}$ in the LC cells, respectively.

3.3. Photosynthetic Ci affinity, photosynthesis, dark respiration and rETR

Photosynthetic affinity for DIC or CO_2 was depressed in the HC cells, as reflected in the relationship of either photosynthesis or rETR (using PAM fluorometer) *v* DIC curves (Fig. 1). The half-saturation concentration ($K_{1/2}$) for both DIC and CO_2 increased

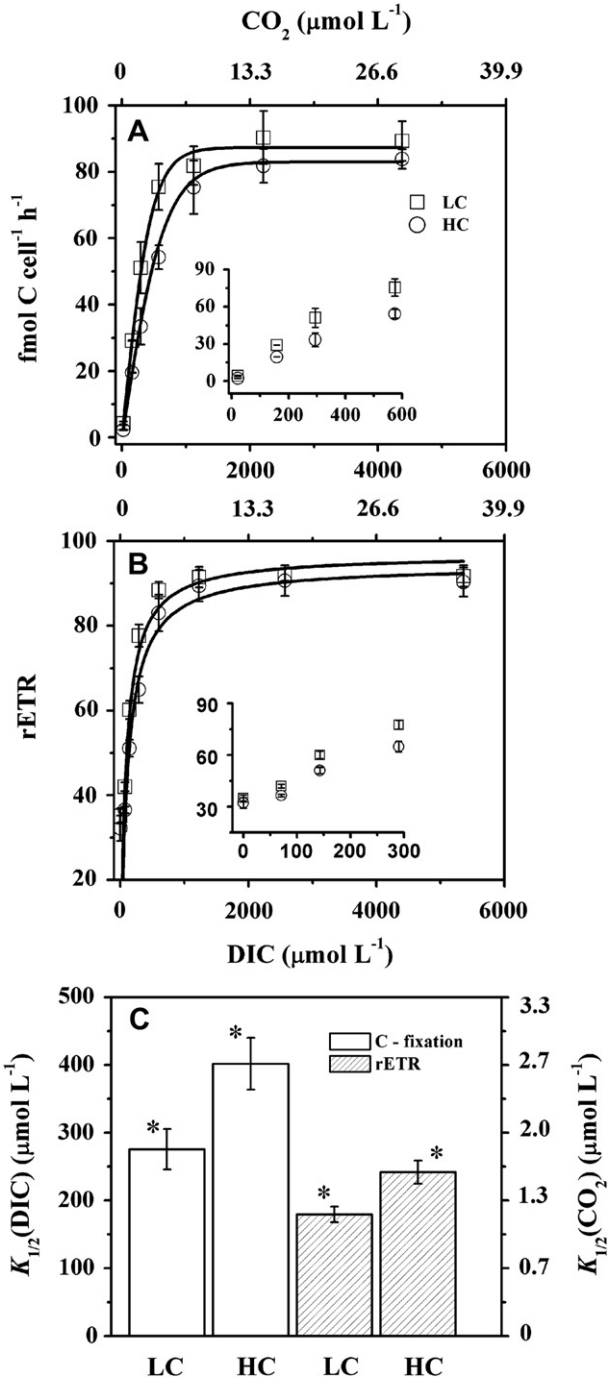

Fig. 1. Photosynthetic carbon fixation rate (A) and rETR (B) as a function of dissolved inorganic carbon (DIC) concentrations, obtained under photon flux densities of 400 μmol photons m^{-2} s^{-1}. Half-saturation constants ($K_{1/2}$) for DIC (C, left) and CO_2 (C, right) were derived from (A) and (B). Both the ambient (low)-CO_2 (LC, 390 μatm, pH = 8.16) and high-CO_2 (HC, 1000 μatm, pH = 7.83) grown cells were measured at the same pH level of 8.16. Asterisks above histogram bars indicate significant difference between LC and HC grown cells at $p = 0.05$ level.

Table 2
The fitted parameters derived from P–I curves and RLCs (i.e., α, the apparent photosynthetic efficiency; P_{max}, the maximum rate of photosynthesis [fmol cell^{-1} h^{-1}] or rETR (a.u.); I_k, the initial light saturation point) of low-CO_2 (LC) and high-CO_2 (HC) grown cells, and of that measured in inversely changed media defined as LC–HC (low-CO_2 grown cells measured in high-CO_2 medium) and HC–LC (high-CO_2 grown cells measured in low-CO_2 medium), respectively. The values are means ± SD of three replicate measurements, derived from Fig. 2A and Fig. 3. The superscripted letters indicate significant difference.

		α	P_{max}	I_k (μmol photons m^{-2} s^{-1})
HC	Photosynthesis	1.20 ± 0.09^{a}	107.03 ± 5.5^{a}	89.5 ± 10.6^{a}
	rETR	0.291 ± 0.007^{c}	131.5 ± 4.0^{c}	451.6 ± 18.7^{c}
LC	Photosynthesis	0.93 ± 0.01^{b}	91.8 ± 3.93^{b}	99.2 ± 5.2^{a}
	rETR	0.295 ± 0.006^{c}	128.2 ± 3.6^{c}	434.4 ± 15.3^{c}
HC–LC	rETR	0.296 ± 0.008^{c}	123.9 ± 3.7^{cd}	419.0 ± 18.7^{cd}
LC–HC	rETR	0.296 ± 0.005^{c}	131.7 ± 3.3^{ce}	444.9 ± 11.4^{ce}

significantly ($p < 0.01$) in the HC cells, by 46% derived from the photosynthesis *v* DIC curves, or by 35% derived from the rETR *v* DIC curves compared to the LC cells (Fig. 1C), reflecting a down-regulation of CCM under the ocean acidification condition. The efficiency of Ci acquisition, the ratio of V_{max} to $K_{1/2}$ for both DIC and CO_2, decreased significantly ($p = 0.03$) in the HC cells, by about 39% and 29% for photosynthetic rates and rETR, respectively. Independent of the different growth CO_2 levels, the maximum rates of photosynthesis and electron transport were unaffected ($p = 0.62$). The V_{max} of photosynthetic carbon fixation and rETR in the HC cells were 82.47 ± 6.32 fmol cell^{-1} h^{-1} and 95.25 ± 4.18 (a.u.), compared to 94.15 ± 14.69 fmol cell^{-1} h^{-1} and 96.54 ± 2.40 (a.u.) in the LC cells. However, both the photosynthetic rates and rETR at limiting DIC levels were significantly lower ($p = 0.03$) in the HC than in the LC cells, by up to 57% and 15% (inset in Fig. 1), respectively, reflecting a higher extent of the rate-limitation by less CO_2 availability under DIC limiting levels in the HC grown cells.

When measured at respective growth CO_2 and pH levels, the HC cells showed higher maximum photosynthetic rate (P_{max}) by 17% and apparent photosynthetic efficiency (α) by 29% (Fig. 2A, Table 2). The HC cells required a lower PAR level (89.5 ± 10.6 μmol photons m^{-2} s^{-1}) than the LC cells (99.2 ± 5.2 μmol photons m^{-2} s^{-1}) to saturate photosynthetic carbon fixation rate, though the difference was not significant ($p = 0.22$) (Table 2).

In view of the RLCs, there was no significant difference in the apparent ETR efficiency (α), P_{max}(rETR) and saturating PAR level (I_k) between HC and LC cells (Table 2, Fig. 3), though significantly lower P_{max}(rETR) and I_k were found in the HC–LC cells (high-CO_2 grown cells measured in low-CO_2 medium) compared to that in the LC–HC cells (low-CO_2 grown cells measured in high-CO_2 medium). The values of I_k derived from RLCs were higher than those derived from the P–I curves (Table 2), about 434.4 ± 15.3 μmol photons m^{-2} s^{-1} for the former and 99.2 ± 5.2 μmol photons m^{-2} s^{-1} for the latter.

Table 3
A comparison of the apparent half-saturation DIC or CO_2 concentrations ($K_{1/2}$) for photosynthesis or growth rate (data marked with a superscripted asterisk) among some marine diatoms grown under different CO_2 concentrations. The values that were indirectly obtained from the published data were indicated as ca. prior to them, and "ND" indicates no data.

Authors	Species and pCO_2	CO_2 (μmol L^{-1}) in cultures	$K_{1/2}$ DIC (μmol L^{-1})	$K_{1/2}$ CO_2 (μmol L^{-1})
Riebesell et al. (1993)	*Ditylum brightwellii*	0.8–95	ND	1.4*
	Thalassiosira punctigera		ND	1.2*
	Rhizosolenia cf. *alata*		ND	2.1*
Burkhardt et al. (2001)	*Thalassiosira weissflogii*	13	ca. 390 ± 70	ND
		67	ca. 510 ± 47	ND
	Phaeodactylum tricornutum	13	ca. 738 ± 107	ND
		67	ca. 1176 ± 120	ND
Matsuda et al. (2001)	*Phaeodactylum tricornutum*	10	71 ± 82	ND
		1615	1009 ± 82	ND
Chen and Gao (2003)	*Skeletonema costatum*	12	203 ± 13	1.2 ± 0.1
		31	241 ± 23	1.4 ± 0.1
Rost et al. (2003)	*Skeletonema costatum*	13	ND	2.3 ± 0.5
		67	ND	2.7 ± 0.4
Trimborn et al. (2008)	*Pseudo-nitzschia multiseries*	9.4	223 ± 39	2.2 ± 0.3
		32	327 ± 57	3.5 ± 0.5
	Nitzschia navis-varingica	9.4	301 ± 84	3.1 ± 0.9
		32	494 ± 67	4.6 ± 0.7
	Stellarima stellaris	9.4	304 ± 84	4.0 ± 0.5
		32	572 ± 133	7.4 ± 1.7
Trimborn et al. (2009)	*Eucampia zodiacus*	14	323 ± 53	2.9 ± 0.4
		30	411 ± 63	3.6 ± 0.5
	Skeletonema costatum	14	265 ± 53	2.8 ± 0.4
		30	441 ± 74	3.1 ± 0.4
	Thalassionema nitzschioides	14	223 ± 41	1.9 ± 0.6
		30	379 ± 78	2.7 ± 0.6
Wu et al. (2010)	*Phaeodactylum tricornutum*	13	525 ± 63	3.6 ± 0.5
		33	621 ± 23	4.2 ± 0.2
This study	*Thalassiosira pseudonana*	13	276 ± 30	1.8 ± 0.2
		33	402 ± 38	2.7 ± 0.2

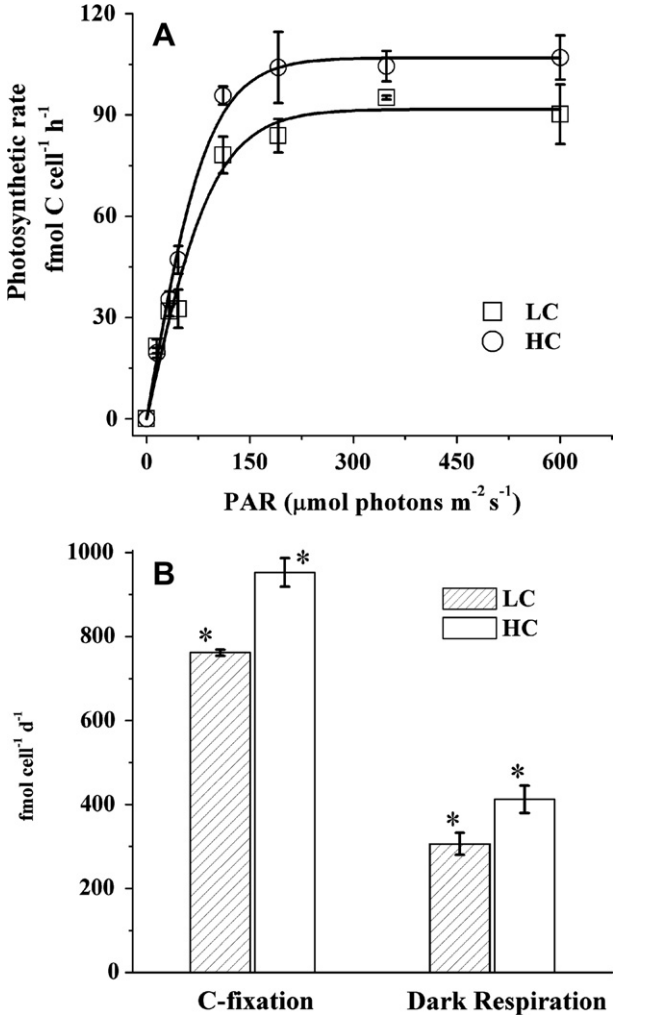

Fig. 2. (A): Photosynthetic carbon fixation rate (fmol C cell^{-1} h^{-1}), measured in their corresponding fresh medium, as a function of irradiance (PAR) for LC (squares) and HC (circles) grown cells. (B): Daily gross carbon fixation (C-fixation) and daily dark respiration for LC and HC grown cells of their sub-saturating growth PAR intensity. Error bars represent means ± SD, $n = 3$ (for triplicate cultures). Asterisks above histogram bars indicate significant difference between HC and LC grown cells at $p = 0.05$ level.

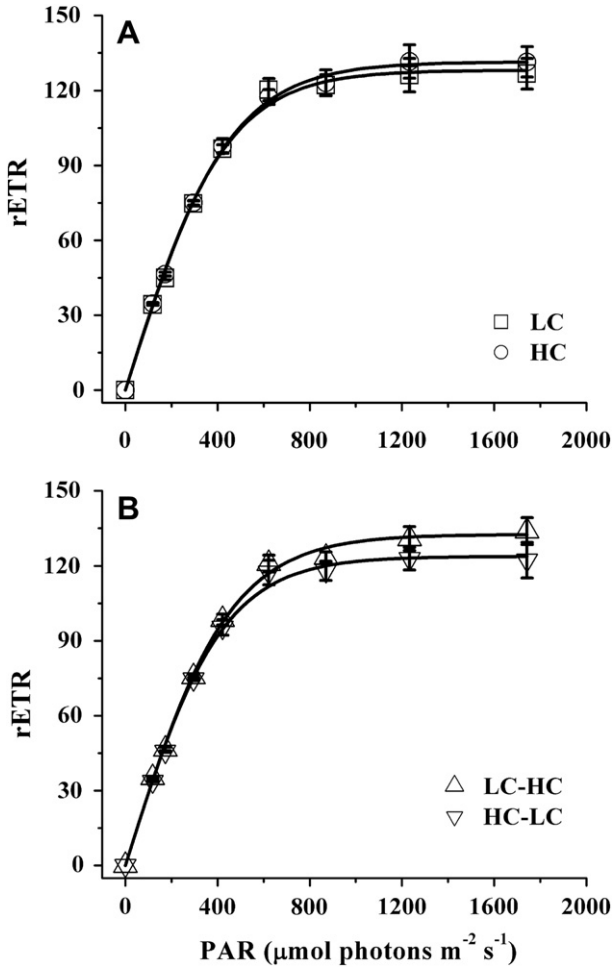

Fig. 3. Rapid light curves of LC (squares) and HC (circles) grown cells (A), and of that measured in inversely changed media defined as LC–HC (low-CO_2 grown cells measured in high-CO_2 medium, up-triangles) and HC–LC (high-CO_2 grown cells measured in low-CO_2 medium, down-triangles) (B), respectively. Error bars represent means ± SD, $n = 3$ (for triplicate cultures).

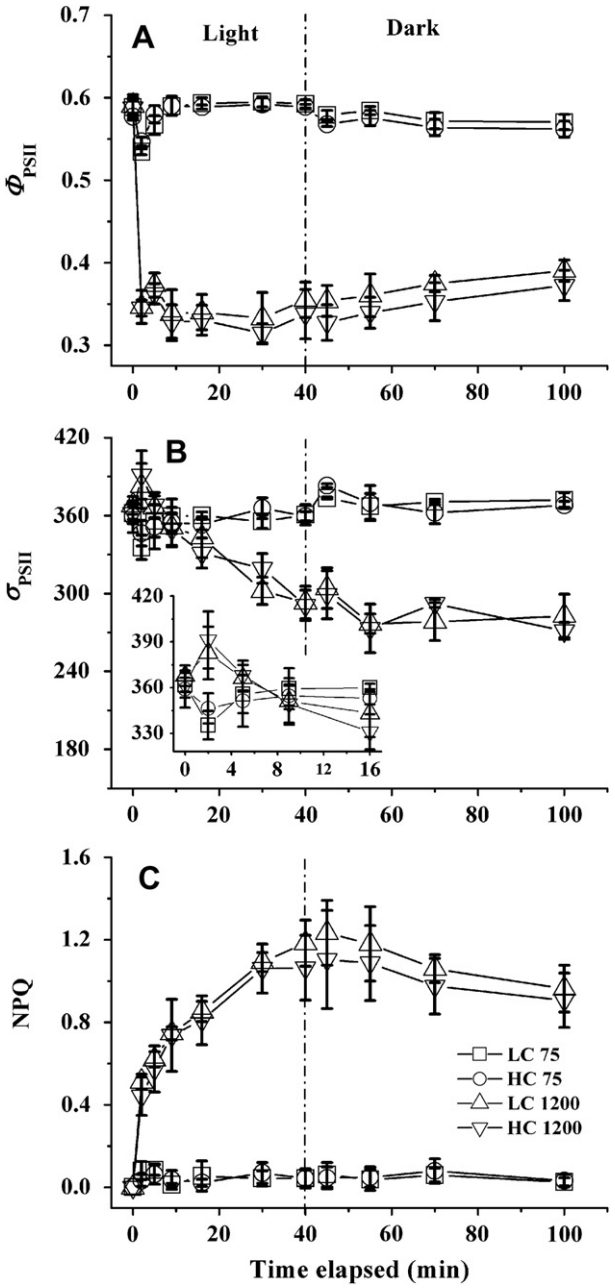

Fig. 4. Time course of the effective quantum yield (Φ_{PSII}) (A), effective absorbance cross-section of PSII (σ_{PSII}) (B) and non-photochemical quenching (NPQ) (C) of LC and HC grown cells. Cell suspensions with cell concentration of ca. 0.5×10^5 cell mL^{-1} were dark adapted for 15 min before exposure to the growth and elevated light intensities (75 and 1200 μmol photons m^{-2} s^{-1}) for 40 min, then recovered in darkness for 60 min. LC, 75 μmol photons m^{-2} s^{-1}, squares; HC, 75 μmol photons m^{-2} s^{-1}, circles; LC, 1200 μmol photons m^{-2} s^{-1}, up-triangles; HC, 1200 μmol photons m^{-2} s^{-1}, down-triangles; the dashed line delineates the light treatment and recovery periods. Error bars represent means ± SD, $n = 3$ (for triplicate cultures).

The photosynthetic carbon fixation rate at the growth light intensity, which was sub-saturating, was much higher ($p = 0.01$) in the HC, by 25% (14.69 ± 2.55 fmol C $cell^{-1}$ h^{-1}), than the LC cells (Fig. 2A). On the other hand, dark respiration rate increased ($p = 0.01$) by 35% (4.42 ± 0.98 fmol O_2 $cell^{-1}$ h^{-1}) in the HC compared to the LC cells. Nevertheless, the daily net photosynthetic production based on the difference of daytime gross carbon fixation and daily respiratory carbon loss was still significantly ($p = 0.01$) higher, by 18% (84.93 ± 4.80 fmol $cell^{-1}$ d^{-1}) in the HC than in the LC cells (Fig. 2B).

3.4. Photoinhibition

The Φ_{PSII}, NPQ and σ_{PSII} were measured using the FIRe when the cells were exposed to a PAR level of 1200 μmol photons m^{-2} s^{-1}, which was well saturating but did not bring about inhibition of ETR during the short exposure (10 s) (Fig. 3). During a longer exposure period (40 min), photoinhibition occurred in both HC and LC cells in view of the changes in the photochemical parameters (Fig. 4). Compared to those exposed to the growth PAR level (75 μmol photons m^{-2} s^{-1}), their Φ_{PSII} declined to 0.35 ± 0.02 (decreased by 42%) in less than 2 min and was then sustained; σ_{PSII} slightly increased in 2 min at the beginning of exposure, and then decreased steadily to 291.9 ± 11.3 (decreased by 20%) in 40 min; NPQ increased to its maximum (1.12 ± 0.14) in 40 min. Following the subsequent dark treatment, Φ_{PSII} increased by 0.04 ± 0.01; NPQ decreased by 0.19 ± 0.08; but σ_{PSII} did not show any recovery. No significant ($p > 0.35$) difference in the photochemical parameters was found between the HC and LC cells either during the high light exposure or dark recovery period, suggesting that seawater acidification did not result in any differential response to light stress in this diatom.

Table 4
Stimulative, unaffected and negative effects of elevated CO_2 concentrations reported in diatoms.

Effects	Authors	Species	Culture condition	Aspects
Stimulative	Riebesell et al. (1993)	*Ditylum brightwellii* *Thalassiosira punctigera* *Rhizosolenia* cf. *alata*	0.8–95 μmol L^{-1} CO_2, PAR at 120 μmol photons m^{-2} s^{-1}	Growth
	Schippers et al. (2004)	*Phaeodactylum tricornutum*	20 μmol L^{-1} CO_2, surface solar PAR at 135 μmol photons m^{-2} s^{-1}	Growth
	Kim et al. (2006)	*Skeletonema costatum*	24 μmol L^{-1} CO_2, mesocosm, solar PAR	Growth
	Wu et al. (2010)	*Phaeodactylum tricornutum*	33 μmol L^{-1} CO_2, PAR at 120 μmol photons m^{-2} s^{-1}	Growth
	King et al. (2011)	*Attheya* sp.	37 μmol L^{-1} CO_2, PAR at 80 μmol photons m^{-2} s^{-1}	Growth
	Low-DÉCarie et al. (2011)	*Navicula pelliculosa*	28 μmol L^{-1} CO_2, PAR at 100 μmol photons m^{-2} s^{-1}	Growth
	Gao et al. (2012)	Diatoms	33 μmol L^{-1} CO_2, ca. 20% solar PAR	Growth
	This study	*Thalassiosira pseudonana*	33 μmol L^{-1} CO_2, PAR at 75 μmol photons m^{-2} s^{-1}	Photosynthesis
Unaffected	Chen and Gao (2003)	*Skeletonema costatum*	31 μmol L^{-1} CO_2, PAR at 210 μmol photons m^{-2} s^{-1}	Growth; Photosynthesis
	Kim et al. (2006)	*Nitzschia* spp.	24 μmol L^{-1} CO_2, mesocosm, solar PAR	Growth
	Boelen et al. (2011)	*Chaetoceros brevis*	40 μmol L^{-1} CO_2, PAR at 70 μmol photons m^{-2} s^{-1}	Growth
	Gao et al. (2012)	Diatoms	33 μmol L^{-1} CO_2, ca. 30% solar PAR	Growth
	This study	*Thalassiosira pseudonana*	33 μmol L^{-1} CO_2, PAR at 75 μmol photons m^{-2} s^{-1}	Growth; Photoinhibition
Negative	Wu et al. (2010)	*Phaeodactylum tricornutum*	33 μmol L^{-1} CO_2, PAR at 120 μmol photons m^{-2} s^{-1}	Photoinhibition; Dark respiration
	Low-DÉCarie et al. (2011)	*Nitzschia palea*	28 μmol L^{-1} CO_2, PAR at 100 μmol photons m^{-2} s^{-1}	Growth
	Gao et al. (2012)	Diatoms	33 μmol L^{-1} CO_2, more than 40% solar PAR	Growth
	Torstensson et al. (2012)	*Navicula directa*	35 μmol L^{-1} CO_2, PAR at 50 μmol photons m^{-2} s^{-1}	Growth
	This study	*Thalassiosira pseudonana*	33 μmol L^{-1} CO_2, PAR at 75 μmol photons m^{-2} s^{-1}	Dark respiration

4. Discussion and conclusion

In the present study, the diatom *T. pseudonana* down-regulated its CCM under 1000 μatm CO_2 and increased its photosynthesis and mitochondrial respiration, leading to insignificant change in growth rate. However, the changed seawater carbonate system did not lead to additional light stress compared to the present seawater state, which contrasts to the previous finding that the diatom *P. tricornutum* grown under the same high-CO_2 level shows inhibited rETR (Wu et al., 2010).

4.1. Inorganic carbon acquisition

There are many types of CCMs in diatoms, differing among different species (Burkhardt et al., 2001; Trimborn et al., 2008, 2009; Wu et al., 2010). *Thalassiosira nitzschioides* (Trimborn et al., 2009), *T. weissflogii* and *P. tricornutum* (Burkhardt et al., 2001) actively take up both CO_2 and HCO_3^-, while *T. punctigera* exclusively use free CO_2 (Elzenga et al., 2000). For *T. pseudonana*, even when there is a lack of eCA, it can take up bicarbonate directly without an anion exchange-type transporter (Elzenga et al., 2000; Nimer et al., 1997). Trimborn et al. (2009) detect low eCA activity in *T. pseudonana*, and show that both eCA and iCA activities are unaffected when the cells are grown at 800 μatm CO_2 for at least 3 days. However, decreased activity of eCA and iCA of *T. weissflogii* and *P. tricornutum* are reported under 1800 μatm CO_2 (Burkhardt et al., 2001). On the other hand, Martin and Tortell (2008) observe a positive correlation between HCO_3^- direct transport and eCA expression in *T. pseudonana*. It appears that *T. pseudonana* can actively transport both CO_2 and HCO_3^-. In the present study, as indicated by the $K_{1/2}$ values, the CCM of *T. pseudonana* was down-regulated by 46% under an elevated CO_2 level of 1000 μatm, reducing the efficiency of Ci acquisition ($V_{max}/K_{1/2}$) by 39%. Such down-regulated CCM might be due to the increased availability of both CO_2 and bicarbonate. However, in another work (Trimborn et al., 2009), the same strain dose not exhibit any down-regulation of its CCM when acclimated to 800 μatm CO_2 for 3 days. The discrepancy from the present work, which grew the cells under 1000 μatm for 15 days (more than 20 generations), might be attributed to the acclimation span or differences in seawater carbonate system. When compared to *P. tricornutum* and other diatoms, in view of the half-saturation concentrations ($K_{1/2}$) of DIC or CO_2, *T. pseudonana* obviously operated a more efficient CCM (Table 3), and 1000 μatm CO_2 (33 μmol L^{-1}) decreased its CCM to a higher extent compared to *P. tricornutum* (46% *v* 18%). While all the diatoms listed in Table 3 down-regulated their CCMs when grown under doubling or higher CO_2 concentrations, *T. pseudonana* was among those that showed the greatest decrease in its photosynthetic affinities for Ci.

4.2. Growth, photosynthesis, respiration, photosynthetic electron transport

Enhanced photosynthetic carbon fixation and mitochondrial respiration were found under ocean acidification conditions in *T. pseudonana* (Fig. 2), and the balance between the enhanced carbon fixation and carbon loss could be responsible for the insignificant change in growth. Stimulated growth and photosynthesis are reported in other diatoms (Table 4) and phytoplankton assemblages (Hein and Sand-Jensen, 1997; Riebesell et al., 2007) of rising CO_2 concentrations, and are attributed to the reduced energetic cost due to the down-regulation of CCM or the increased availability of CO_2. However, other studies show insignificant effects (Boelen et al., 2011; Chen and Gao, 2003; Nielsen et al., 2012, 2010; Tortell et al., 2002; Tortell and Morel, 2002) and even negative effects (Feng et al., 2009; Low-DÉCarie et al., 2011; Torstensson et al., 2012) on photosynthesis, growth or primary productivity in diatoms or phytoplankton community. These discrepancies appear to be related to the balance between the stimulative and negative (additional carbon loss) effects associated with increased CO_2 and seawater acidity, although species-specific differences and experimental conditions might also affect the net outcome (Table 4). Our recent study show that the combination of rising CO_2 and increased light exposure reduced primary productivity in the diatom-dominated areas (Gao et al., 2012). The experimental conditions in the present study and those of Wu et al. (2010) were almost the same except for the growth light intensities (Table 4). However, while the growth rate in the previous study testing *P. tricornutum* was stimulated but not in the present study testing *T. pseudonana* at the same elevated CO_2 level, the 60% difference in the light level could be responsible, since *T. pseudonana* showed more than 100% higher light use efficiency than *P. tricornutum* (Gao et al., 2012,

Supplementary information). *P. tricornutum* lacks eCA and takes CO_2 as its major Ci source (Burkhardt et al., 2001), therefore, it can easily benefit from increased availability of CO_2. Increased dark respiration under ocean acidification conditions (Wu et al., 2010 and the present study) might play a role in counteracting external pH reduction and providing the additional energy demand for maintaining internal acid-base stability. Other physiological pathways, such as photorespiration of *T. pseudonana* was enhanced under the ocean acidification condition by about 23% (Gao et al., 2012), which was also observed in *Symbiodinium Acropora formosa* (Crawley et al., 2010). Enhanced excretion of organic compounds due to photorespiration links to stimulated production of transparent exopolymers (Engel, 2002). These metabolic pathways could result in discrepant effects of ocean acidification on different species or under different light levels.

The relationship between electron transport and light (the RLC) can hardly be interpreted as traditional P–I curve, since the short exposure (10 s for each increment of light level) cannot ensure full acclimation to a given PAR (Hawes et al., 2003), leading to large differences in the saturating light levels (I_k) between these two models. In fact, not all of the electrons transported from PSII are used for carbon assimilation; non-assimilatory electron transport may be used for active transport of CO_2 or HCO_3^- (Li and Canvin, 1998; Sültemeyer et al., 1993), or for the reduction of oxygen to run the water–water cycle (Asada, 2000) or for photorespiration (Heber et al., 1996). Thus, in our study, a much higher I_k was observed in RLCs than in the P–I curves (Table 2). In *T. pseudonana*, the HC and LC grown cells exhibited equal amounts of electron transfer, but less of them were used for carboxylation in the LC grown cells (Fig. 2A). This "less energy use" efficiency was also shown in lower apparent photosynthetic carbon fixation efficiency per quantum (Table 2). This suggests that extra electron flow is expended to operate the CCM (Li and Canvin, 1998; Sültemeyer et al., 1993). The HC and LC cells responded differentially to the abrupt changes in the carbonate system when shifted inversely (Fig. 3B), reflecting their immediate physiological response to the chemical changes.

4.3. Photoinhibition

No significant difference in cellular content of pigments and σ_{PSII} was found between HC and LC grown cells, reflecting their equal capability for light energy capture. Decreasing σ_{PSII} and increasing dissipation of excessive light energy (i.e. NPQ) are effective strategies for phytoplankton to withstand high levels of PAR (Falkowski and Owens, 1980; Niyogi et al., 2005). *T. pseudonana* employed these strategies to cope with light stress (Fig. 4). The HC and LC grown cells did not show any inhibition in electron transport rates at high PAR levels up to 1800 μmol photons m^{-2} s^{-1} during the short exposures for the RLCs determination (Fig. 3), but showed significant photoinhibition under elongated exposures to 1200 μmol photons m^{-2} s^{-1} of PAR (Fig. 4). The initial several increments of light during the RLC determination might have led ATPase and Calvin cycle enzymes to a highly activated state, generating a trans-thylakoid pH gradient to control the fast component of NPQ (qE, as described by Krause and Weis, 1991). Thus, exposure to high PAR for 10 s appeared not to result in photoinhibition. In contrast, the longer exposure to the high PAR level would de-activate ATPase and Calvin cycle enzymes due to the prior 15 min dark adaptation (Arana et al., 1986; MacIntyre et al., 1997). Besides, full qE activation requires approximately 10–15 min under a saturating photo flux (Niyogi et al., 1998) and, therefore, photoinhibition would easily occur during this elongated exposure. Accordingly, photoinhibition in *T. pseudonana* seemed to be dose-dependent rather than PAR intensity-dependent.

The efficiency with which CCMs operate in *P. tricornutum* and *T. pseudonana* could be down-regulated under the CO_2 level projected for the end of this century (Wu et al., 2010; this study). In *T. pseudonana*, the HC and LC grown cells showed identical photochemical inhibition during the exposures to the high PAR (Fig. 4), reflecting that high light tolerance was not influenced under ocean acidification conditions. In contrast, electron transport of *P. tricornutum* was more inhibited by exposing the HC grown cells to supersaturating PAR (1200 μmol photons m^{-2} s^{-1}) (Wu et al., 2010). Such differential responses between these two diatoms suggested that species-specific mechanisms were involved in coping with the combined impacts of ocean acidification and light stress. Photochemical responses to light stress under ongoing ocean acidification may differ in different diatom species due to the diversified metabolic pathways they use to cope with changed seawater chemistry and fluctuating solar radiation. In the present study, down-regulated photosynthetic affinity for DIC or CO_2 might be partially related to the down-regulated activity of PEPCase, which shows high affinity for HCO_3^-, since the activities of PEPCase and PEPCKase in *T. pseudonana* and their transcription might decrease under high-CO_2 conditions (Reinfelder et al., 2000). A decreased ratio of CO_2 to O_2 near Rubisco due to down-regulated CCM and/or PEPCase could enhance oxygenation and photorespiration, which are known to play photoprotective roles (Wingler et al., 2000). In *T. pseudonana*, high-CO_2 grown cells showed a 23% increase in photorespiration (Gao et al., 2012), which might aid in counteracting the increased acidity and light stress, therefore leading to similar photoinhibition as in the LC grown cells, although the down-regulation of CCM might result in additional light stress.

Acknowledgments

This study was supported by the National Basic Research Program of China (No. 2009CB421207 and 2011CB200902), the National Natural Science Foundation (No. 40930846, No. 41120164007), the Programs for Changjiang Scholars and Innovative Research Team (IRT0941) and the China–Japan collaboration project from MOST (S2012GR0290). We thank Dr. Yaping Wu for his technical advice, Yahe Li for her kind assistance during the experiment, and Prof. John Hodgkiss for reading and correcting the English in this manuscript.

References

Arana, J.L., Gianni, H., Ravizzini, R.A., Vallejos, R.H., 1986. The deactivation process of the proton-ATPase in isolated chloroplasts and whole leaves. Biochimica et Biophysica Acta (BBA)-Bioenergetics 850, 294–299.

Armbrust, E.V., Berges, J.A., Bowler, C., Green, B.R., Martinez, D., Putnam, N.H., Zhou, S.G., Allen, A.E., Apt, K.E., Bechner, M., Brzezinski, M.A., Chaal, B.K., Chiovitti, A., Davis, A.K., Demarest, M.S., Detter, J.C., Glavina, T., Goodstein, D., Hadi, M.Z., Hellsten, U., Hildebrand, M., Jenkins, B.D., Jurka, J., Kapitonov, V.V., Kröger, N., Lau, W.W.Y., Lane, T.W., Larimer, F.W., Lippmeier, J.C., Lucas, S., Medina, M., Montsant, A., Obornik, M., Parker, M.S., Palenik, B., Pazour, G.J., Richardson, P.M., Rynearson, T.A., Saito, M.A., Schwartz, D.C., Thamatrakoln, K., Valentin, K., Vardi, A., Wilkerson, F.P., Rokhsar, D.S., 2004. The genome of the diatom *Thalassiosira pseudonana*: ecology, evolution, and metabolism. Science 306, 79–86.

Asada, K., 2000. The water-water cycle as alternative photon and electron sinks. Philosophical Transactions of the Royal Society of London Series B: Biological Sciences 355, 1419–1431.

Badger, M.R., Andrews, T.J., Whitney, S.M., Ludwig, M., Yellowlees, D.C., Leggat, W., Price, G.D., 1998. The diversity and coevolution of Rubisco, plastids, pyrenoids, and chloroplast-based CO_2-concentrating mechanisms in algae. Canadian Journal of Botany-Revue Canadienne de Botanique 76, 1052–1071.

Beardall, J., Burger-Wiersma, T., Rijkeboer, M., Sukenik, A., Lemoalle, J., Dubinsky, Z., Fontvielle, D., 1994. Studies on enhanced post-illumination respiration in microalgae. Journal of Plankton Research 16, 1401–1410.

Boelen, P., Van De Poll, W.H., Van Der Strate, H.J., Neven, I.A., Beardall, J., Buma, A.G.J., 2011. Neither elevated nor reduced CO_2 affects the photophysiological performance of the marine Antarctic diatom *Chaetoceros brevis*. Journal of Experimental Marine Biology and Ecology 406, 38–45.

Bouma, T., Visser, R.D., Janssen, J., Kock, M.J.D., Leeuwen, P.H.V., Lambers, H., 1994. Respiratory energy requirements and rate of protein turnover in vivo determined by the use of an inhibitor of protein synthesis and a probe to assess its effect. Physiologia Plantarum 92, 585–594.

Burkhardt, S., Amoroso, G., Riebesell, U., Sültemeyer, D., 2001. CO_2 and HCO_3^- uptake in marine diatoms acclimated to different CO_2 concentrations. Limnology and Oceanography 46, 1378–1391.

Cai, W.J., Wang, Y.C., 1998. The chemistry, fluxes, and sources of carbon dioxide in the estuarine waters of the Satilla and Altamaha Rivers, Georgia. Limnology and Oceanography 43, 657–668.

Caldeira, K., Wickett, M.E., 2003. Anthropogenic carbon and ocean pH. Nature 425, 365.

Chen, X.W., Gao, K.S., 2003. Effect of CO_2 concentrations on the activity of photosynthetic CO_2 fixation and extracelluar carbonic anhydrase in the marine diatom *Skeletonema costatum*. Chinese Science Bulletin 48, 2616–2620.

Crawley, A., Kline, D.I., Dunn, S., Anthony, K., Dove, S., 2010. The effect of ocean acidification on symbiont photorespiration and productivity in *Acropora formosa*. Global Change Biology 16, 851–863.

Dickson, A.G., 1990. Standard potential of the reaction: $AgCl(s) + ½\ H_2(g) = Ag(s) + HCl(aq)$, and the standard acidity constant of the ion HSO_4^- in synthetic seawater from 273.15 to 318.15 K. The Journal of Chemical Thermodynamics 22, 113–127.

Elzenga, J.T.M., Prins, H.B.A., Stefels, J., 2000. The role of extracellular carbonic anhydrase activity in inorganic carbon utilization of *Phaeocystis globosa* (Prymnesiophyceae): a comparison with other marine algae using the isotopic disequilibrium technique. Limnology and Oceanography 45, 372–380.

Engel, A., 2002. Direct relationship between CO_2 uptake and transparent exopolymer particles production in natural phytoplankton. Journal of Plankton Research 24, 49–53.

Falkowski, P.G., Koblížek, M., Gorbunov, M., Kolber, Z., 2004. Development and application of variable chlorophyll fluorescence techniques in marine ecosystems. In: Papageorgiou, G.C., Govindjee (Eds.), Chlorophyll a Fluorescence: a Signature of Photosynthesis. Springer, Dordrecht, pp. 757–778.

Falkowski, P.G., Owens, T.G., 1980. Light-shade adaptation: two strategies in marine phytoplankton. Plant Physiology 66, 592–595.

Feng, Y.Y., Hare, C.E., Leblanc, K., Rose, J.M., Zhang, Y.H., DiTullio, G.R., Lee, P.A., Wilhelm, S.W., Rowe, J.M., Sun, J., Nemcek, N., Gueguen, C., Passow, U., Benner, I., Brown, C., Hutchins, D.A., 2009. Effects of increased pCO_2 and temperature on the North Atlantic spring bloom. I. The phytoplankton community and biogeochemical response. Marine Ecology Progress Series 388, 13–25.

Gao, K.S., Wu, Y.P., Li, G., Wu, H.Y., Villafañe, V.E., Helbling, E.W., 2007. Solar UV radiation drives CO_2 fixation in marine phytoplankton: a double-edged sword. Plant Physiology 144, 54–59.

Gao, K.S., Xu, J.T., Gao, G., Li, Y.H., Hutchins, D.A., Huang, B.Q., Wang, L., Zheng, Y., Jin, P., Cai, X.N., Häder, D.P., Li, W., Xu, K., Liu, N.N., Riebesell, U., 2012. Rising CO_2 and increased light exposure synergistically reduce marine primary productivity. Nature Climate Change. http://dx.doi.org/10.1038/NCLIMATE1507.

Gordillo, F.J.L., Jiménez, C., Chavarría, J., Xavier Niell, F., 2001. Photosynthetic acclimation to photon irradiance and its relation to chlorophyll fluorescence and carbon assimilation in the halotolerant green alga *Dunaliella viridis*. Photosynthesis Research 68, 225–235.

Hawes, I., Sutherland, D., Hanelt, D., 2003. The use of pulse amplitude modulated fluorometry to determine fine-scale temporal and spatial variation of in situ photosynthetic activity within an isoetes-dominated canopy. Aquatic Botany 77, 1–15.

Heber, U., Bligny, R., Streb, P., Douce, R., 1996. Photorespiration is essential for the protection of the photosynthetic apparatus of C_3 plants against photoinactivation under sunlight. Botanica Acta 109, 307–315.

Hein, M., Sand-Jensen, K., 1997. CO_2 increases oceanic primary production. Nature 388, 526–527.

Holm-Hansen, O., Helbling, E.W., 1995. Técnicas para la medición de la productividad primaria en el fitoplancton. In: Alveal, K., Ferrario, M.E., Oliveira, E.C., Sar, E. (Eds.), Manual de Métodos Ficológicos. Universidad de Concepción, Concepción, Chile, pp. 329–350.

Hopkinson, B.M., Dupont, C.L., Allen, A.E., Morel, F.M.M., 2011. Efficiency of the CO_2-concentrating mechanism of diatoms. Proceedings of the National Academy of Sciences 108, 3830–3837.

Ihnken, S., Eggert, A., Beardall, J., 2010. Exposure times in rapid light curves affect photosynthetic parameters in algae. Aquatic Botany 93, 185–194.

IPCC, 2001. Climate change 2001: the scientific basis. In: Houghton, J.T., et al. (Eds.), Contribution of Working Group I to the Third Assessment Report of the Intergovernmental Panel on Climate Change. Cambridge University Press, Cambridge.

Jassby, A.D., Platt, T., 1976. Mathematical formulation of the relationship between photosynthesis and light for phytoplankton. Limnology and Oceanography 21, 540–547.

Kim, J.M., Lee, K., Shin, K., Kang, J.H., Lee, H.W., Kim, M., Jang, P.G., Jang, M.C., 2006. The effect of seawater CO_2 concentration on growth of a natural phytoplankton assemblage in a controlled mesocosm experiment. Limnology and Oceanography 51, 1629–1636.

King, A.L., Sañudo-Wilhelmy, S.A., Leblanc, K., Hutchins, D.A., Fu, F.X., 2011. CO_2 and vitamin B_{12} interactions determine bioactive trace metal requirements of a subarctic Pacific diatom. The ISME Journal 5, 1388–1396.

Kramer, D.M., Cruz, J.A., Kanazawa, A., 2003. Balancing the central roles of the thylakoid proton gradient. Trends in Plant Science 8, 27–32.

Krause, G., Weis, E., 1991. Chlorophyll fluorescence and photosynthesis: the basics. Annual Review of Plant Biology 42, 313–349.

Lewis, E., Wallace, D.W.R., 1998. Program Developed for CO_2 System Calculations. ORNL/CDIAC-105. Carbon Dioxide Information Analysis Center, Oak Ridge National Laboratory. US Department of Energy, Oak Ridge, Tennessee.

Li, Q., Canvin, D.T., 1998. Energy sources for HCO_3^- and CO_2 transport in air-grown cells of *Synechococcus* UTEX 625. Plant Physiology 116, 1125–1132.

Lloyd, S.W., Tucker, C.S., 1988. Comparison of three solvent systems for extraction of chlorophyll a from fish pond phytoplankton communities. Journal of the World Aquaculture Society 19, 36–40.

Low-DÉCarie, E., Fussmann, G.F., Bell, G., 2011. The effect of elevated CO_2 on growth and competition in experimental phytoplankton communities. Global Change Biology 17, 2525–2535.

MacIntyre, H.L., Sharkey, T.D., Geider, R.J., 1997. Activation and deactivation of ribulose-1,5-bisphosphate carboxylase/oxygenase (Rubisco) in three marine microalgae. Photosynthesis Research 51, 93–106.

Martin, C.L., Tortell, P.D., 2008. Bicarbonate transport and extracellular carbonic anhydrase in marine diatoms. Physiologia Plantarum 133, 106–116.

Matsuda, Y., Hara, T., Colman, B., 2001. Regulation of the induction of bicarbonate uptake by dissolved CO_2 in the marine diatom, *Phaeodactylum tricornutum*. Plant, Cell & Environment 24, 611–620.

Milligan, A.J., Mioni, C.E., Morel, F.M.M., 2009. Response of cell surface pH to pCO_2 and iron limitation in the marine diatom *Thalassiosira weissflogii*. Marine Chemistry 114, 31–36.

Morel, F.M.M., Rueter, J.G., Anderson, D.M., Guillard, R.R.I., 1979. Aquil: a chemically defined phytoplankton culture medium for trace metal studies. Journal of Phycology 15, 135–141.

Nielsen, L.T., Hallegraeff, G.M., Wright, S.W., Hansen, P.J., 2012. Effects of experimental seawater acidification on an estuarine plankton community. Aquatic Microbial Ecology 65, 271–285.

Nielsen, L.T., Jakobsen, H.H., Hansen, P.J., 2010. High resilience of two coastal plankton communities to twenty-first century seawater acidification: evidence from microcosm studies. Marine Biology Research 6, 542–555.

Nimer, N.A., Iglesias-Rodriguez, M.D., Merrett, M.J., 1997. Bicarbonate utilization by marine phytoplankton species. Journal of Phycology 33, 625–631.

Niyogi, K.K., Grossman, A.R., Björkman, O., 1998. Arabidopsis mutants define a central role for the xanthophyll cycle in the regulation of photosynthetic energy conversion. The Plant Cell Online 10, 1121–1134.

Niyogi, K.K., Li, X.P., Rosenberg, V., Jung, H.S., 2005. Is PsbS the site of non-photochemical quenching in photosynthesis? Journal of Experimental Botany 56, 375–382.

Reinfelder, J.R., Kraepiel, A.M.L., Morel, F.M.M., 2000. Unicellular C_4 photosynthesis in a marine diatom. Nature 407, 996–999.

Reinfelder, J.R., Milligan, A.J., Morel, F.M.M., 2004. The role of the C_4 pathway in carbon accumulation and fixation in a marine diatom. Plant Physiology 135, 2106–2111.

Riebesell, U., Schulz, K.G., Bellerby, R.G.J., Botros, M., Fritsche, P., Meyerhöfer, M., Neill, C., Nondal, G., Oschlies, A., Wohlers, J., Zöllner, E., 2007. Enhanced biological carbon consumption in a high CO_2 ocean. Nature 450, 545–548.

Riebesell, U., Tortell, P.D., 2011. Effects of ocean acidification on pelagic organisms and ecosystems. In: Gattuso, J.P., Hansson, L. (Eds.), Ocean Acidification. Oxford University Press, NewYork, pp. 291–311.

Riebesell, U., Wolf-Gladrow, D.A., Smetacek, V., 1993. Carbon dioxide limitation of marine phytoplankton growth rates. Nature 361, 249–251.

Ritchie, R.J., 2006. Consistent sets of spectrophotometric chlorophyll equations for acetone, methanol and ethanol solvents. Photosynthesis Research 89, 27–41.

Rost, B., Riebesell, U., Burkhardt, S., Sültemeyer, D., 2003. Carbon acquisition of bloom-forming marine phytoplankton. Limnology and Oceanography 48, 55–67.

Roy, R.N., Roy, L.N., Vogel, K.M., Porter-Moore, C., Pearson, T., Good, C.E., Millero, F.J., Campbell, D.M., 1993. The dissociation constants of carbonic acid in seawater at salinities 5 to 45 and temperature 0 to 45 °C. Marine Chemistry 44, 249–267.

Sültemeyer, D., Biehler, K., Fock, H.P., 1993. Evidence for the contribution of pseudocyclic photophosphorylation to the energy requirement of the mechanism for concentrating inorganic carbon in *Chlamydomonas*. Planta 189, 235–242.

Schippers, P., Lürling, M., Scheffer, M., 2004. Increase of atmospheric CO_2 promotes phytoplankton productivity. Ecology Letters 7, 446–451.

Silverman, D.N., 1991. The catalytic mechanism of carbonic anhydrase. Canadian Journal of Botany 69, 1070–1078.

Sukenik, A., Tchernov, D., Kaplan, A., Huertas, E., Lubian, L.M., Livne, A., 1997. Uptake, efflux, and photosynthetic utilization of inorganic carbon by the marine Eustigmatophyte *Nannochloropsis* sp. Journal of Phycology 33, 969–974.

Tchernov, D., Hassidim, M., Luz, B., Sukenik, A., Reinhold, L., Kaplan, A., 1997. Sustained net CO_2 evolution during photosynthesis by marine microorganism. Current Biology 7, 723–728.

Torstensson, A., Chierici, M., Wulff, A., 2012. The influence of increased temperature and carbon dioxide levels on the benthic/sea ice diatom *Navicula directa*. Polar Biology 35, 205–214.

Tortell, P.D., DiTullio, G.R., Sigman, D.M., Morel, F.M.M., 2002. CO_2 effects on taxonomic composition and nutrient utilization in an equatorial Pacific phytoplankton assemblage. Marine Ecology Progress Series 236, 37–43.

Tortell, P.D., Morel, F.M.M., 2002. Sources of inorganic carbon for phytoplankton in the eastern subtropical and equatorial Pacific Ocean. Limnology and Oceanography 47, 1012–1022.

Tortell, P.D., Rau, G.H., Morel, F.M.M., 2000. Inorganic carbon acquisition in coastal Pacific phytoplankton communities. Limnology and Oceanography 45, 1485–1500.

Trimborn, S., Lundholm, N., Thoms, S., Richter, K.U., Krock, B., Hansen, P.J., Rost, B., 2008. Inorganic carbon acquisition in potentially toxic and non-toxic diatoms: the effect of pH-induced changes in seawater carbonate chemistry. Physiologia Plantarum 133, 92–105.

Trimborn, S., Wolf-Gladrow, D.A., Richter, K.U., Rost, B., 2009. The effect of pCO_2 on carbon acquisition and intracellular assimilation in four marine diatoms. Journal of Experimental Marine Biology and Ecology 376, 26–36.

Wingler, A., Lea, P.J., Quick, W.P., Leegood, R.C., 2000. Photorespiration: metabolic pathways and their role in stress protection. Philosophical Transactions of the Royal Society of London Series B: Biologic 355, 1517–1529.

Wu, Y.P., Gao, K.S., Riebesell, U., 2010. CO_2-induced seawater acidification affects physiological performance of the marine diatom *Phaeodactylum tricornutum*. Biogeosciences 7, 2915–2923.

Xu, Z.G., Gao, K.S., 2009. Impacts of UV radiation on growth and photo synthetic carbon acquisition in *Gracilaria lemaneiformis* (Rhodophyta) under phosphorus-limited and replete conditions. Functional Plant Biology 36, 1057–1064.